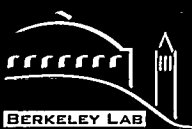


10/12/96 8:50

BNL-39162  
UC-1501



# ERNEST ORLANDO LAWRENCE BERKELEY NATIONAL LABORATORY

## *In Situ* Spectroscopic Applications to the Study of Rechargeable Lithium Batteries

Y. Gofer, R. Barbour, Y. Luo, I.T. Bae, L.-F. Li,  
and D.A. Scherson

**Energy and Environment Division**

May 1996



#### **DISCLAIMER**

This document was prepared as an account of work sponsored by the United States Government. While this document is believed to contain correct information, neither the United States Government nor any agency thereof, nor The Regents of the University of California, nor any of their employees, makes any warranty, express or implied, or assumes any legal responsibility for the accuracy, completeness, or usefulness of any information, apparatus, product, or process disclosed, or represents that its use would not infringe privately owned rights. Reference herein to any specific commercial product, process, or service by its trade name, trademark, manufacturer, or otherwise, does not necessarily constitute or imply its endorsement, recommendation, or favoring by the United States Government or any agency thereof, or The Regents of the University of California. The views and opinions of authors expressed herein do not necessarily state or reflect those of the United States Government or any agency thereof, or The Regents of the University of California.

Available to DOE and DOE Contractors  
from the Office of Scientific and Technical Information  
P.O. Box 62, Oak Ridge, TN 37831  
Prices available from (615) 576-8401

Available to the public from the  
National Technical Information Service  
U.S. Department of Commerce  
5285 Port Royal Road, Springfield, VA 22161

Ernest Orlando Lawrence Berkeley National Laboratory  
is an equal opportunity employer.

**IN SITU SPECTROSCOPIC APPLICATIONS TO THE  
STUDY OF RECHARGEABLE LITHIUM BATTERIES**

Final Report

July 1996

by

**Yosi Gofer  
Rachael Barbour  
Yuyan Luo  
In Tae Bae  
Lin-Feng Li  
Daniel A. Scherson**

Department of Chemistry  
Case Western Reserve University  
Cleveland, Ohio 44106-7078

for

Exploratory Technology Research Program  
Energy & Environment Division  
Lawrence Berkeley National Laboratory  
Berkeley, California 94720-0001

This work was supported by the Assistant Secretary for Energy Efficiency and Renewable Energy, Office of Transportation Technologies, Office of Advanced Automotive Technologies of the U.S. Department of Energy under Contract No. DE-AC03-76SF00098, Subcontract No. 4606210 with the Ernest Orlando Lawrence Berkeley National Laboratory.

DISTRIBUTION OF THIS DOCUMENT IS UNLIMITED

*ng* **MASTER**



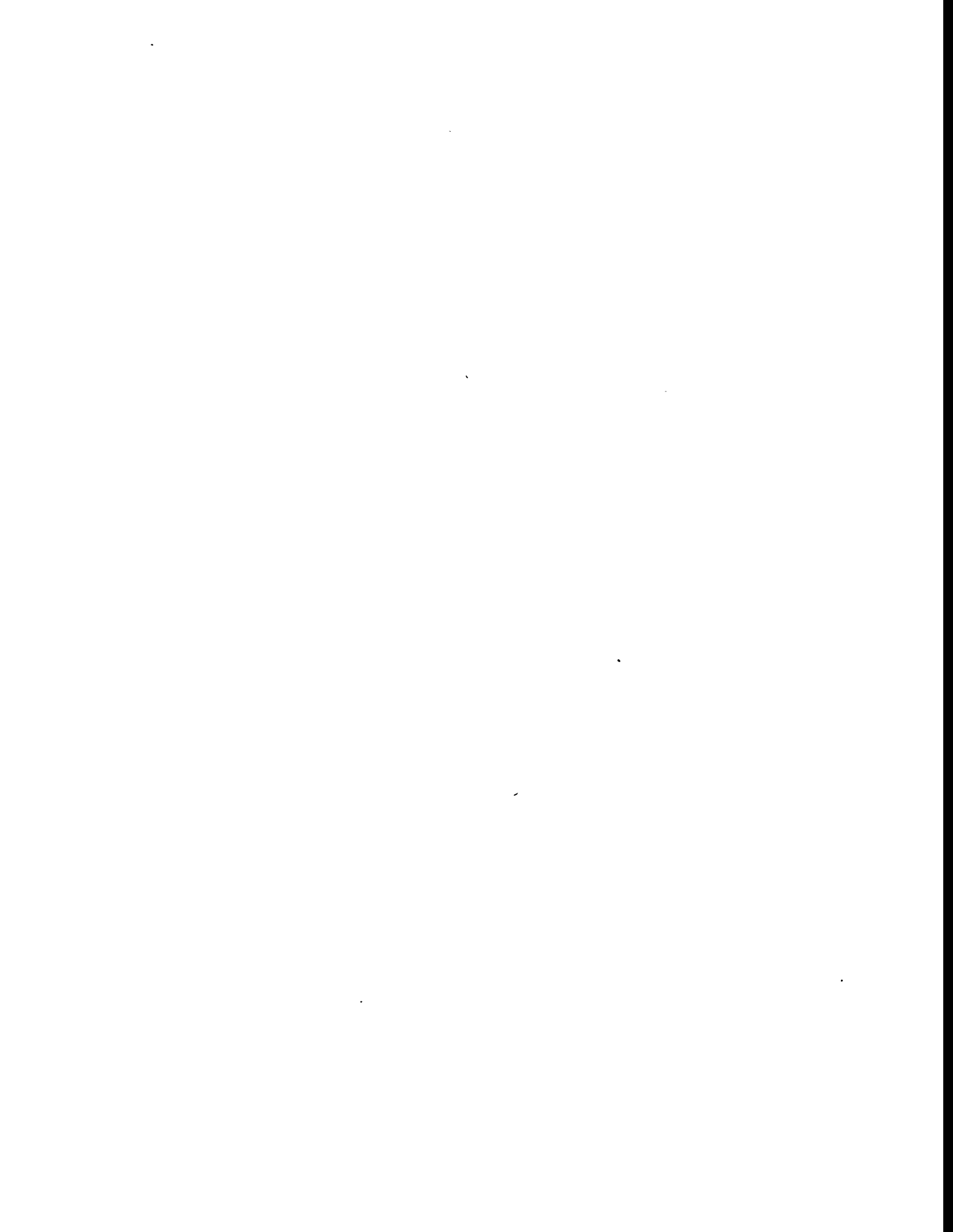
## **DISCLAIMER**

**Portions of this document may be illegible  
in electronic image products. Images are  
produced from the best available original  
document.**

## ELECTROCHEMISTRY IN ULTRAHIGH VACUUM

### TABLE OF CONTENTS

|  |    |
|--|----|
| ABSTRACT.....  | v  |
| I. INTRODUCTION.....   | 1  |
| II. EXPERIMENTAL.....  | 2  |
| a. Ultrahigh Vacuum Chamber.....                               | 3  |
| b. Cleaning and Characterization of Electrodes in UHV.....     | 3  |
| c. Ultrapurification of poly(ethylene oxide) .....             | 4  |
| d. Preparation of PEO/LiClO <sub>4</sub> Films.....            | 5  |
| e. Electrochemical Instrumentation.....                        | 5  |
| f. Electrochemical Cell for Measurements in the Glove Box..... | 5  |
| g. Electrochemical Cell for Measurements in UHV.....           | 6  |
| h. Two-, versus three-electrode cell arrangement.....          | 7  |
| i. Other Experimental Considerations.....                      | 7  |
| III. RESULTS AND DISCUSSION .....                              | 8  |
| A. Intercalation of Li <sup>+</sup> into HOPG(bp).....         | 8  |
| B. Li UPD on Au.....   | 11 |
| IV. CONCLUDING REMARKS.....                                    | 15 |
| V. REFERENCES.....   | 16 |
| VI. FIGURE CAPTIONS.....                                       | 16 |



## ABSTRACT

A new experimental approach has been developed and implemented for the study of various aspects of lithium electrochemistry under utmost conditions of cleanliness. This novel strategy takes advantage of the low vapor pressure of ultrapure lithium salt/polyethylene oxide electrolytes for conducting conventional electrochemical experiments in ultrahigh vacuum environments with a wide variety of electrodes prepared and characterized by surface analytical techniques. Two processes were investigated using a LiClO<sub>4</sub>/PEO electrolyte at temperatures in the range of 55 - 70°C:

- i) Electrochemical insertion of lithium into the basal plane of highly ordered pyrolytic graphite, HOPG(bp).
- ii) Underpotential deposition (UPD) of Li onto polycrystalline Au.

The results provided conclusive evidence (except for impurity effects) that the electrochemical behavior observed in UHV is indeed characteristic of the systems selected for these studies, and therefore, is not affected in any discernible way by the ultralow pressures.

In the case of Li UPD on polycrystalline Au, the voltammetric curves were similar to those observed in liquid non-aqueous solvent electrolytes, displaying deposition and stripping peaks with a charge equivalent to the adsorption and desorption of a single Li<sup>+</sup> per surface site.

## I. INTRODUCTION

The advent of solid polymeric materials displaying high ionic conductivities at relatively low temperatures has opened new prospects for improved electrical energy storage and energy generation devices.<sup>1</sup> Recent efforts in battery technology have focused on the study of solid organic polymers capable of transporting lithium ions, but impervious to attack by metallic lithium.<sup>2</sup> Highly promising is polyethylene oxide (PEO),<sup>3</sup> a material that shows moderate Li<sup>+</sup>-ion conductivities at temperatures as low as 55°C, even in the absence of co-solvents or other additives.

During *in situ* characterization of the short-term stability of ultrapurified PEO-based electrolytes toward metallic Li using Attenuated Total Reflection-Fourier Transform Infrared (ATR-FTIR) Spectroscopy, spectroelectrochemical measurements were performed at reduced pressure, on the order of a fraction of a Pa.<sup>4</sup> Such an approach was successful in decreasing the effects associated with gas phase contaminants, *without modifying the overall electrochemical response*. Prompted by the possibility of conducting such experiments under even lower pressures, the degassing properties of ultrapurified PEO, LiClO<sub>4</sub> and LiClO<sub>4</sub>/PEO films were investigated using a turbo molecular pump, and ultimately, an ion-pumped chamber equipped with a mass spectrometer. The presence of the PEO or LiClO<sub>4</sub>/PEO films in the main chamber produced no observable increase in the base pressure of the system, indicating that the degassing rate of PEO was less than ca. 10<sup>-7</sup> Pa·l/s·cm<sup>2</sup> even at temperatures as high as 70 ± 5°C. This finding is important, as it identifies LiClO<sub>4</sub>/PEO as an ideal electrolyte for carrying out a variety of conventional electrochemical experiments in ultrahigh vacuum (UHV). This environment not only provides experimental conditions of utmost cleanliness, but enables the characterization of highly reactive electrochemically prepared interfaces with an array of powerful

electron-based spectroscopies without the use of elaborate systems to transfer specimens from a high-pressure auxiliary chamber to the main UHV chamber, as is the case with aqueous electrochemistry.

This report presents results for electrochemical experiments performed in UHV using a LiClO<sub>4</sub>/PEO solid polymer electrolyte involving:

- i) the electrochemical insertion of lithium into the basal plane of highly ordered pyrolytic graphite, HOPG(bp).
- ii) the underpotential deposition of Li on polycrystalline (poly) Au.

The interest in these specific systems stems from the following considerations. Lithium-intercalation carbon electrodes are the most promising anodes for rechargeable lithium-battery applications.<sup>3,5</sup> In addition to their improved safety characteristics and ease of manufacturing, the overall morphology of many of these materials is not largely affected by their state of charge (amount of lithium in the lattice). This behavior is unlike that observed with metallic lithium, which during recharge develops dendrites, or other fibrillar deposits, which can perforate the separator leading to internal shorts.<sup>6</sup> Furthermore the studies involving gold electrodes are expected to provide much needed insight into fundamental aspects of elementary reactions at the metal/solid polymer electrolyte interface.

All experiments described herein were performed at 55 ± 5°C with a simple two-electrode electrochemical cell, using a lithium foil as the counter/reference electrode (Li[C/R]) and a film of ultrapurified LiClO<sub>4</sub>/PEO as the solid polymer electrolyte.

## II. EXPERIMENTAL

### a. Ultrahigh Vacuum Chamber

Electrochemical measurements conducted in UHV were carried out in a custom-design chamber (MC, Varian) operating at pressures on the order of  $2 \times 10^{-8}$  Pa (1 Pa =  $7.5 \cdot 10^{-3}$  torr), with hydrogen, water, carbon monoxide and carbon dioxide as the main constituents. This system is equipped with a single-pass cylindrical mirror analyzer (CMA, Varian 981-2607) with a coaxial electron gun (Varian 981-2613) for acquisition of the Auger electron (AES) spectra, and a Dycor mass spectrometer to analyze residual gases (not shown in the figure). One port in the MC is connected via a gate valve (GV1, see Fig. 1) to an independently pumped antechamber which contains a magnetically coupled manipulator (MCM1) for insertion and retrieval of specimens into and from MC without exposure to the atmosphere. A ceramic nipple (CN) was interposed between MCM1 and the antechamber to isolate electrically the lithium foil counter-reference electrode (see below) from the working electrode. Both the HOPG(bp) and Au(poly) were mounted on the specially designed holders that enable transfer of specimens in and out of MC under UHV conditions.

### b. Cleaning and Characterization of Electrodes in UHV

The HOPG(bp) working electrode (Advanced Ceramics Corp., Parma, OH), was a square wafer of ca.  $1 \text{ cm}^2$  area, cleaved with a razor knife to form a circular protruding section of about  $0.7 \text{ cm}^2$  (see Insert B, Fig. 1). Two electrically isolated Ta strips were used to resistively heat the HOPG during the cleaning procedure (up to 1000 K) and the electrochemical experiments (up to 325 K). The temperature was monitored with a K-type alumel/chromel thermocouple junction inserted on the side of the HOPG(bp) (not shown in the figure) and controlled manually by adjusting the output of

the power supply. Electrical connection to the HOPG was achieved with a wire (not shown in the figure) spot welded to a  $0.10\text{ cm}^2$  piece of Ta trapped between the circular mica spacer and the back of the specimen (not shown in the figure). Just before transferring the HOPG specimen to the main chamber, a fresh, clean HOPG basal plane was exposed by cleaving the surface with adhesive tape. A series of heating cycles were performed up to 1000 K to remove water and oxygen from the HOPG(bp) as evidenced by AES.

The Au(poly) electrode was mounted on the same special holder (see above) and cleaned by a series of  $\text{Ar}^+$ -sputtering, and occasionally, thermal annealing cycles until the AES spectra displayed features characteristic of clean metallic Au with only minor contributions (<1% AES signal) from oxygen and carbon impurities.

Auger electron spectra were recorded in the derivative mode (5 V peak-to-peak modulation at 17 kHz) with the electron beam (3 keV  $\pm$  10eV at  $5 \pm 1\text{ }\mu\text{A}$ ) normal to the specimen.

#### c. Ultrapurification of poly(ethylene oxide)

Poly(ethylene oxide) (PEO) (Aldrich, 600,000 molecular weight) was purified by dialysis to remove calcium (ca. 0.003%) derived from traces of the polymerization initiator (calcium amide) and other impurities. The cellulose dialysis bags (Sigma. Chem. Co.), were cleaned by first rinsing with distilled water followed by boiling in an ethanol/water mixture (1:1) for one hour and finally rinsing again with distilled water. The PEO was placed in the bags and dialyzed in water for 48 hours, changing the solvent every 2-3 hours the first day, and every 4-5 hours the second day. After this procedure was completed the PEO/water solution was evaporated to dryness in a Rotavap.

#### d. Preparation of PEO/LiClO<sub>4</sub> Films

Poly(ethylene oxide) film electrolytes were prepared with ultrapurified PEO/LiClO<sub>4</sub> acetonitrile solutions as described elsewhere,<sup>7</sup> except that the films were dried in a vacuum dessicator equipped with heating capabilities installed inside a high-quality glove box (Vacuum Atmospheres) with oxygen and humidity sensors. A calibrated Variac and a thermocouple were used to set the appropriate temperature. In this fashion, the PEO films are never exposed to the ambient atmosphere.

#### e. Electrochemical Instrumentation

All electrochemical experiments were conducted either with a Pine potentiostat (UHV) or a EG&G Princeton Applied Research Potentiostat Model 273 (glove box). Voltammetric cycles were always initiated at or near the open circuit potential (OCP) at scan rates in the range 5 - 20 mV/sec.

#### f. Electrochemical Cell for Measurements in the Glove Box

Cyclic voltammetry curves obtained in the glove box were recorded using a specially designed electrochemical cell consisting of a series of components in a sandwich-type arrangement. The working electrode was a Au film sputtered on a glass slide (ca. 100-200 nm thick). A polyethylene (PE) gasket, 50  $\mu$ m thick, cut in the form of a frame (16 mm x 50 mm, outer, and 9 mm x 40 mm, inner dimensions) was then laid down on the gold-coated substrate followed by a (8 mm x 39 mm) PEO(LiClO<sub>4</sub>) electrolyte film positioned in the center of the PE gasket. The counter electrode was a piece of lithium ribbon (0.3 mm x 12 mm x 45 mm) placed over the SPE with its edges in the boundaries of the PE gasket. To complete the cell, a nickel-coated glass slide or current collector was placed directly in contact with the lithium ribbon.

Prior to the experimental measurements, the cell was compressed between a flat aluminum plate that was lined with a porous, flexible polymer-based material and a stainless steel plate. An etched foil element encapsulated in Kapton (Omegalux Kapton Insulated Flexible Heaters, ca. 0.25 mm x 12.7 mm x 51 mm) was mounted on both plates. The temperature was monitored with a thermocouple (J-type) inserted into the aluminum plate, next to the nickel-coated glass and controlled (within 1 to 2 degrees) using an Omega CN4400 controller.

#### g. Electrochemical Cell for Measurements in UHV

The Li[C/R]/PEO(LiClO<sub>4</sub>) arrangement involved in the UHV electrochemical experiments (see Insert A, Fig. 1) was assembled in the glove box. The Li[C/R] was a small circular foil of freshly scraped metallic Li pressed against the flat end of a stainless steel holder (SSH), which was then covered by a circular piece of ultrapure LiClO<sub>4</sub>(PEO) film that was tightly held with a small stainless steel (SS) clamp.

The SSH was screwed onto the end of a long magnetically coupled manipulator (MCM2) and then isolated from the glovebox atmosphere with a UHV-quality gate valve (GV2). This transfer chamber was then removed from the glovebox and attached to a nipple (N) connected via a gate valve (GV3) to the antechamber. After evacuation, the Li[C/R](PEO)/SSH was transferred from MCM1 to MCM2 using a second tapped hole in SSH with the PEO/Li foil facing the UHV chamber port normal to the MCM1 axis. A schematic diagram of SSH with the two attached MCM's is shown in Insert B, Fig. 1. In this fashion, the electrochemical cell was easily formed by translating MCM1 into the main UHV chamber and placing the PEO/Li assembly directly parallel and against the HOPG(bp) surface. A schematic diagram of the assembled cell is shown in Insert B, Fig. 1.

#### h. Two-, versus three-electrode cell arrangement

A few measurements were performed in the glove box to examine the behavior of a two-electrode cell, like the one involved in the UHV experiments (see above), with that of a three-electrode cell. For these experiments, a section of the slide described in Section f, was isolated electrically from the rest of the evaporated gold film by mechanically removing a ca. 50  $\mu\text{m}$  wide strip. After the cell was assembled and heated, lithium was electrodeposited on one section of the gold film (using the Li foil as a counter electrode) which was used as a reference electrode. Experiments involving the deposition and stripping of bulk Au indicated that, except for a shift in potential, there are no differences between the results obtained using the same cell in the three-electrode or two-electrode mode (see Fig. 2).

#### i. Other Experimental Considerations

Once the sandwich-type electrochemical cell was assembled, it was heated to the desired temperature allowing several minutes for the overall system to stabilize before data acquisition was initiated. Except where otherwise noted, all potentials are reported with respect to the Li[C/R]. Although electrochemical measurements were performed over the range 50 - 80°C, only results obtained at 60°C and 75°C are presented here.

Cyclic voltammograms of clean Au (before Li UPD) recorded in UHV were obtained from different sections of the *same* Au(poly) specimen *after a single cleaning cycle*, taking advantage of the fact that the PEO/Li[C/R]] electrode is much smaller in diameter than the Au foil.

### III. RESULTS AND DISCUSSION

#### A. Intercalation of $\text{Li}^+$ into HOPG(bp)

The AES spectra of HOPG(bp) obtained after the thermal treatment, immediately before the  $\text{Li}[\text{C/R}]/\text{PEO}(\text{LiClO}_4)$  assembly was introduced into the main chamber (see Curve A, Fig. 3) displayed features characteristic of graphitic carbon with a small amount of oxygen. After the cell was formed and the temperature had reached  $55^\circ\text{C}$ , a series of cyclic voltammograms was acquired. A curve representative of the *first and subsequent cycles* at  $80 \text{ mV/s}$  is given in curve A, Fig. 4. As shown therein, currents associated with the intercalation of lithium in HOPG(bp) were observed at potentials more negative than  $1.25 \text{ V}$  vs  $\text{Li}[\text{C/R}]$  with no evidence for *staging*.<sup>8</sup> This behavior is characteristic of HOPG(bp) both in liquid and solid electrolytes. The prominent peak obtained in the scan in the positive direction upon reversing the cycle at  $1.4 \text{ V}$  can be attributed to the deintercalation of Li from the HOPG lattice. Essentially identical features were found in parallel experiments conducted with a sandwich-type cell involving the same constituents in the glove box, as shown in curve B, Fig. 4. This provides unambiguous evidence that the electrochemical behavior observed in UHV is indeed characteristic of the  $\text{Li}/\text{LiClO}_4(\text{PEO})/\text{HOPG}(\text{bp})$  system and is not affected in any discernible way by the ultralow pressures.

Regardless of whether  $\text{Li}^+$ -intercalation into HOPG(bp) from ultraclean PEO/ $\text{LiClO}_4$  films was performed in UHV or in a glove box, the very first linear voltammetric scan in the negative direction (initiated at the open circuit potential) yielded no features at potentials more positive than the onset of lithium intercalation. This provides evidence that the films are free of adventitious water, oxygen and/or carbon dioxide. The charge associated with the first scan in the negative direction, for the HOPG(bp)/PEO( $\text{LiClO}_4$ ) system in both environments, was always larger than

that observed upon reversing the scan at the negative limit, an effect that became less pronounced as the cycling was continued. For example, experiments performed in the glove box at 5 mV/s in the potential range 0.03 - 3.0 V vs Li/Li<sup>+</sup> with a three-electrode cell yielded values of  $\eta = Q_{deint}/Q_{int}$ , where  $Q_{int}$  and  $Q_{deint}$  represent the charge during intercalation and deintercalation, respectively, of 7.5 % in the first cycle ( $Q_{int} = 26.8 \mu\text{C}/\text{cm}^2$ ,  $Q_{deint} = 74 \mu\text{C}/\text{cm}^2$ ) up to 71.5% in the nineth cycle ( $Q_{int} = 171 \mu\text{C}/\text{cm}^2$ ,  $Q_{deint} = 475 \mu\text{C}/\text{cm}^2$ ). For much faster scan rates, such as those shown in Curve A, Fig. 4,  $\eta$  values as high as 92.5% could be observed in the third cycle.

A charge imbalance during the first charging cycle, also known as the *irreversible capacity loss*, is found during electrochemical lithium intercalation in carbon materials in liquid electrolytes. Such a phenomenon, which adversely affects battery performance, has been attributed, to among other factors, the formation of a film at the interface derived from irreversible reactions between intercalated lithium and the electrolyte, including both the salt and the solvent. Based on the *in situ* ATR/FTIR experiments referred to above, film formation in PEO/LiClO<sub>4</sub> solutions is not likely responsible for the observed charge imbalance; instead, this effect appears to originate from kinetic hindrances during discharge, which prevent the complete deintercalation of lithium from the HOPG(bp) within the time scale of the cyclic voltammetry experiments. Measurements aimed at elucidating this interesting phenomenon are currently in progress in this laboratory and will reported shortly.

Experiments performed in the UHV system, in which the potential was first held at 0.03 V vs Li[C/R] followed by a potential scan at 80 mV/s, in the positive direction up to 3.0 V yielded, within the time scale of the

voltammetric scan, a value of  $Q_{deint}$  of about  $11 \mu\text{A}/\text{cm}^2$ , which decreased monotonically in continuous subsequent cycles between the two voltage limits. Under the experimental conditions employed in this study, the steady-state lithium intercalation currents at  $0.03 \text{ V}$  vs  $\text{Li}[\text{C}/\text{R}]$  were on the order of only a few  $\mu\text{A}/\text{cm}^2$ .

No attempts were made to conduct variable angle take-off AES/XPS or depth profiling to determine spectroscopically the depth of penetration of Li into the HOPG lattice. Long-term experiments in which the HOPG(bp) was polarized for about three days at a potential just positive to lithium bulk deposition, however, did produce in some regions a distinct golden color characteristic of  $\text{LiC}_6$ , which persisted for over one day in the glove box. After carefully removing a layer no thicker than a few microns, the exposed surface was that of bare HOPG(bp) without visual signs of Li intercalation. Although largely qualitative, these observations suggest that Li ions do not diffuse very far, nor very fast into the HOPG lattice.

Immediately after recording this series of voltammograms, the HOPG(bp) was polarized at ca.  $30 \text{ mV}$  vs  $\text{Li}[\text{C}/\text{R}]$ . After a few minutes the cell was disassembled under potential control, by simply retracting MCMI. This process may be regarded as equivalent to a procedure known as *emersion* in liquid electrolytes. No signs of carbon or PEO was observed by visual inspection of the PEO or HOPG(bp) surface, respectively. The presence of lithium in the HOPG lattice was clearly identified by the appearance of a  $43 \text{ eV}$  AES peak in the spectra recorded at  $48^\circ\text{C}$  while the specimen was cooling down to room temperature (see Curve B, Fig. 3).

A quantitative analysis of this AES spectra, based on the homogeneous attenuation model, indicates that the total AES signal associated with oxygen, chlorine, sulfur and nitrogen is below 8%. According to these data, the relative amount of oxygen to chlorine, corrected by their respective

sensitivity factors, is close to 4 to 1. Since chlorine is not found in the pristine HOPG(bp) specimens, the oxygen and chlorine was attributed to a trace of perchlorate ion from  $\text{LiClO}_4$  on the HOPG surface. As is well known, perchlorate ions are labile to reduction by electron and X-ray beams; hence, the presence of chlorine on the surface is understandable. Both nitrogen and sulfur, at very low levels, were found in the majority of HOPG(bp) specimens examined in this laboratory before lithium intercalation and therefore are not derived from the electrolyte. The fact that the total amount of impurities is so low is not consistent with the presence of a film of any significant thickness on the  $\text{Li}^+$ -intercalated/HOPG(bp) surface following emersion. It seems possible that a reaction takes place between the intercalated HOPG(bp) and the PEO/ $\text{LiClO}_4$  film to yield a chemically modified polymeric material that becomes an integral part of the electrolyte. However, *in situ* attenuated total reflection Fourier transform infrared spectroscopy experiments specifically aimed at detecting film formation at ultrapure PEO/ $\text{LiClO}_4$ -Au-coated germanium electrodes interfaces, yielded no spectral features other than those attributed to the polymer electrolyte itself, even when the electrode was polarized at a potential negative enough for bulk lithium deposition to ensue. Therefore, our results are consistent with the view that, within the time scale of these experiments, ultrapure PEO/ $\text{LiClO}_4$  films are impervious to chemical attack by intercalated lithium into carbon.

#### B. Li UPD on Au

Fig. 5 shows the AES spectrum of a fresh Au foil (never exposed to Li) acquired after heavy  $\text{Ar}^+$ -sputtering without subsequent thermal annealing. This spectrum displays minor features due to C (271 eV), N(392 eV), and O (511 eV) in addition to the characteristic Au peaks. The first cyclic

voltammogram obtained for this clean surface immediately after transferring the PEO/Li counter electrode to the UHV chamber and assembling the electrochemical cell is given in Fig. 6. The scan was started at the measured open circuit potential (ca. 2.0 V vs Li[C/R]) at a rate of 16 mV/s. Despite the *tilt* due to uncompensated IR drop, this curve bears some resemblance to those reported in non-aqueous liquid electrolytes in this and other laboratories, and as will be shown later, to those obtained in PEO( $\text{LiClO}_4$ ) in the glove box (see below). Particularly noteworthy, however, is the rather featureless character of the *first* (and subsequent) scan(s) in the negative direction in the range between 1 and 2 V. This behavior is unlike that observed in the *first* scan of Au in other (mostly liquid) electrolytes, *including the same type of PEO/LiClO<sub>4</sub> film in a high quality glovebox*, which exhibit pronounced peaks in this voltage range ascribed to the reduction of adventitious dioxygen and water in the electrolyte. It may thus be concluded, that under the UHV conditions in which these experiments were performed and to the level of sensitivity of cyclic voltammetry, the PEO films are free from water and/or dioxygen impurities.

The peak centered at 0.76 V in the *first* (and subsequent) scan(s) in the negative direction are attributed to the UPD of Li on Au(poly).<sup>12</sup> The increase in the current at more negative potentials is due to the incipient Li/Au alloy formation, which is followed at ca. 0.1 V by Li bulk deposition, as signaled by the characteristic nucleation/growth loop. Evidence for alloy formation was also obtained from virtually identical UHV experiments involving UPD of Li on Ni, a metal that does not form an alloy with Li. As will be shown elsewhere,<sup>13</sup> no monotonic increase in the (negative) current was observed in such case up to the onset of Li bulk deposition.

The peaks observed at the most negative potentials, upon reversing the scan, correspond to the dissolution of the alloy(s) with some contribution due to bulk Li.<sup>12</sup> The last feature centered at 0.97 V observed in the scan in the positive direction is due to the stripping of the UPD Li layer.

Further evidence for the complementary character of the UPD peaks was obtained by reversing the scan in the negative direction at a potential more positive than that required for Li bulk deposition. This is illustrated in Fig. 7, which gives a voltammogram obtained with the same surface at 70°C at a scan rate of 10 mV/s. It is significant that under these conditions the UPD and stripping peaks are displaced by less than 0.1 V as opposed to several tenths of a volt as is often the case in other liquid media. A possible explanation for this phenomenon is the presence of a passive layer generated via the reaction of both Li UPD and metallic lithium with liquid non-aqueous electrolytes and impurities, which would hinder kinetically the UPD process leading to larger peaks separations. In the case of PEO, however, passive layers of such type are not believed to be formed.

Since the area of contact is not accurately known, because of the difficulties in placing the two electrodes perfectly parallel to each other, it is not possible to determine reliably the charge density associated with the UPD features based solely on the voltammogram. However, an accurate estimate of the area of electrochemical contact is made after depositing Li to the equivalent of few thousands of monolayers just prior to opening the cell, and measuring the clearly defined gray imprint left on the electrode surface. For the experimental results shown in this work, this value was of ca. 0.06 cm<sup>2</sup>. Assuming a roughness factor of one, the charge density associated with the UPD peak determined from a straightforward integration of the peak and using reasonable backgrounds (see dashed line in the figure) yielded a value of ca. 210  $\mu$ C/cm<sup>2</sup> for deposition and ca. 170  $\mu$ C/cm<sup>2</sup> for

stripping. Within experimental error, and given the approximate character of this analysis, these values are in fairly good agreement with those expected from the discharge of one electron per Au surface site ( $220 \mu\text{C}/\text{cm}^2$ ), providing evidence that the interfacial process can be indeed ascribed to Li UPD and stripping.

The results shown in Fig. 6 are remarkably similar to those obtained for the same type of PEO/LiClO<sub>4</sub> film (after a few cycles) in a glovebox at 55°C under one atmosphere pressure of an inert gas (see Fig. 8). This observation supports the claims made recently in this laboratory regarding the intercalation of lithium into HOPG(bp) from the same type of PEO-based electrolyte, i.e. the UHV environment does not affect the overall electrochemical behavior of the interface recorded at atmospheric pressures.

Further proof of the conventional character of the electrochemical response of the cell in UHV is given in Fig. 9, which shows a voltammetric curve recorded at 50 mV/s at potentials between -0.5 and 2.5 V. The features observed are characteristic of Li bulk deposition and stripping in this media and are nearly identical to those obtained at atmospheric pressure in the glove box (see Fig. 2).

The melting point of neat (salt-free) PEO films prepared in this fashion determined by differential scanning calorimetry is ca. 55 - 60°C;<sup>14</sup> therefore, some of the measurements presented herein were performed, in the strict sense, in a liquid electrolyte.

#### IV. CONCLUDING REMARKS

In summary, the results demonstrate that a LiClO<sub>4</sub>/PEO solid polymer electrolyte exhibits sufficiently low volatility and stable physicochemical properties to enable conventional electrochemical experiments to be performed in ultrahigh vacuum (UHV). This finding opens new possibilities

for the study of highly reactive electrochemical interfaces with PEC under optimal conditions of cleanliness, without the need of transferring specimens from an auxiliary high-pressure chamber, as is the case with aqueous or other liquid phase electrolytes.

Two areas are expected to constitute the main focus of future research:

- i) the development of new model systems for lithium intercalation into carbon-based materials, including the UHV synthesis of graphite onto nickel substrates using CO and/or ethylene as a precursor.
- ii) a systematic study of the UPD of Li on a wide variety of substrates, such as Cu, Au, Ag, Pt, Ni and Al. The latter material is of considerable interest as Li/Al anodes are being regarded as potential substitutes for metallic lithium in ambient-temperature rechargeable batteries.

#### V. REFERENCES

1. For general reviews in this area see:

*Applications of Electroactive Polymers*, Scrosati, B., Ed. Chapman Hall, New York, 1993.

2. A collection of articles in the area of polymer electrolytes may be found in *Electrochim. Acta* 1992, 37.

3. Abraham, K. M. *Electrochim. Acta* 1993, 38, 1233

4. Zhuang, G.; Wang, K.; Chottiner, G.; Barbour, R.; Luo, Y.; Bae, I. T.; Tryk, D.; Scherson, D. *J. Power Sources* 1995, 54, 20

5. Tarascon, J. M.; Guyomard, D. *Electrochim. Acta* 1993, 38, 1221.

6. Scrosati, B. *J. Electrochem. Soc.* 1992, 139, 2776

7. Ichino, T.; Cahan, B. D.; Scherson, D. A. *J. Electrochem. Soc.* 1991, 138, L59.

8. Dahn, J. R.; Sleigh, A. K.; Shi, H.; Reimers, J. N.; Zhong, Q.; Way, B. *M. Electrochim. Acta* 1993, 38, 1179

9. Wagner, D.; Gerischer, H. *Electrochim. Acta* 1989, 34, 1351
10. Gerischer, H.; Wagner, D. *Ber. Bunsenges. Phys. Chem.* 1988, 92, 1325
11. Li, J.; Pons, S.; Smith, J. J. *Langmuir* 1986, 2, 297
12. Aurbach, D.; Daroux, M.; Faguy, P.; Yeager, E. B. *J. Electroanal. Chem.* 1991, 297, 225.
13. Gofer, Y.; Li, L-F; Chottiner, G.S; Scherson, D.A. (in preparation)
14. Wilson, D. J.; Nicholas, C. V.; Mobbs, R. H.; Booth, C. *British Polymer Journal* 1990, 22, 129.

## VI. FIGURE CAPTIONS

Fig. 1. Schematic diagram of the UHV/antechamber/transfer chamber system for electrochemical measurements involving solid polymer electrolytes. Insert A provides an exploded view of the HOPG(bp) sample holder and Li[C/R]/PEO(LiClO<sub>4</sub>) stainless steel holder (SSH) arrangement attached to both magnetically coupled manipulators. Insert B shows the details of the assembled HOPG(bp)/PEO(LiClO<sub>4</sub>) cell in the UHV chamber. MCM: magnetically coupled manipulator; GV: gate valve; N: nipple; CN: ceramic nipple; SSH: stainless steel holder; TMP: turbomolecular pump.

Fig. 2. Comparison between the cyclic voltammograms with a two (dashed line) and a three (solid line) electrode cell for deposition and stripping of Li from a PEO(LiClO<sub>4</sub>) electrolyte at 55°C. Scan rate: 5 mV/s.

Fig. 3. Comparison between the AES spectra of HOPG(bp) obtained after the thermal treatment, immediately before the Li[C/R]/PEO(LiClO<sub>4</sub>) assembly was introduced into the main chamber (curve A) and after electrochemical intercalation of Li<sup>+</sup> (curve B see text for details).

Fig. 4. Comparison between the cyclic voltammogram for intercalation and deintercalation of  $\text{Li}^+$  from PEO( $\text{LiClO}_4$ ) in UHV and in a high quality glovebox at 55°C. Scan rate: 80 mV/s. The difference in the current scales is due to the higher area of contact for the cell in the glovebox i.e.  $0.75 \text{ cm}^2$  versus  $0.04-0.06 \text{ cm}^2$  in UHV.

Fig. 5. Auger electron spectra of a Au foil after heavy  $\text{Ar}^+$ -sputtering without subsequent thermal annealing.

Fig. 6. First cyclic voltammogram for clean Au foil described in Fig. 5 in UHV in a PEO( $\text{LiClO}_4$ ) electrolyte using a Li counter reference  $\text{Li}[\text{C/R}]$  electrode. The scan was started at the open circuit potential (ca. 2.0 V vs  $\text{Li}[\text{C/R}]$ ) at a rate of 16 mV/s.

Fig. 7. Cyclic voltammogram for the Au(poly) electrode described in caption Fig. 5, in a PEO( $\text{LiClO}_4$ ) electrolyte in UHV at 70°C. Scan rate: 10 mV/s. Other conditions are given in the caption Fig. 6.

Fig. 8. Typical steady state voltammogram obtained for Au(poly) in PEO/ $\text{LiClO}_4$  in a glove box under a 1 atm. pressure of an inert gas at 55°C. Scan rate: 5 mV/s.

Fig. 9. Cyclic voltammetry of Au(poly) in PEO( $\text{LiClO}_4$ ) electrolyte in UHV showing characteristic features attributed to bulk deposition and stripping of Li. Scan rate: 50 mV/s.

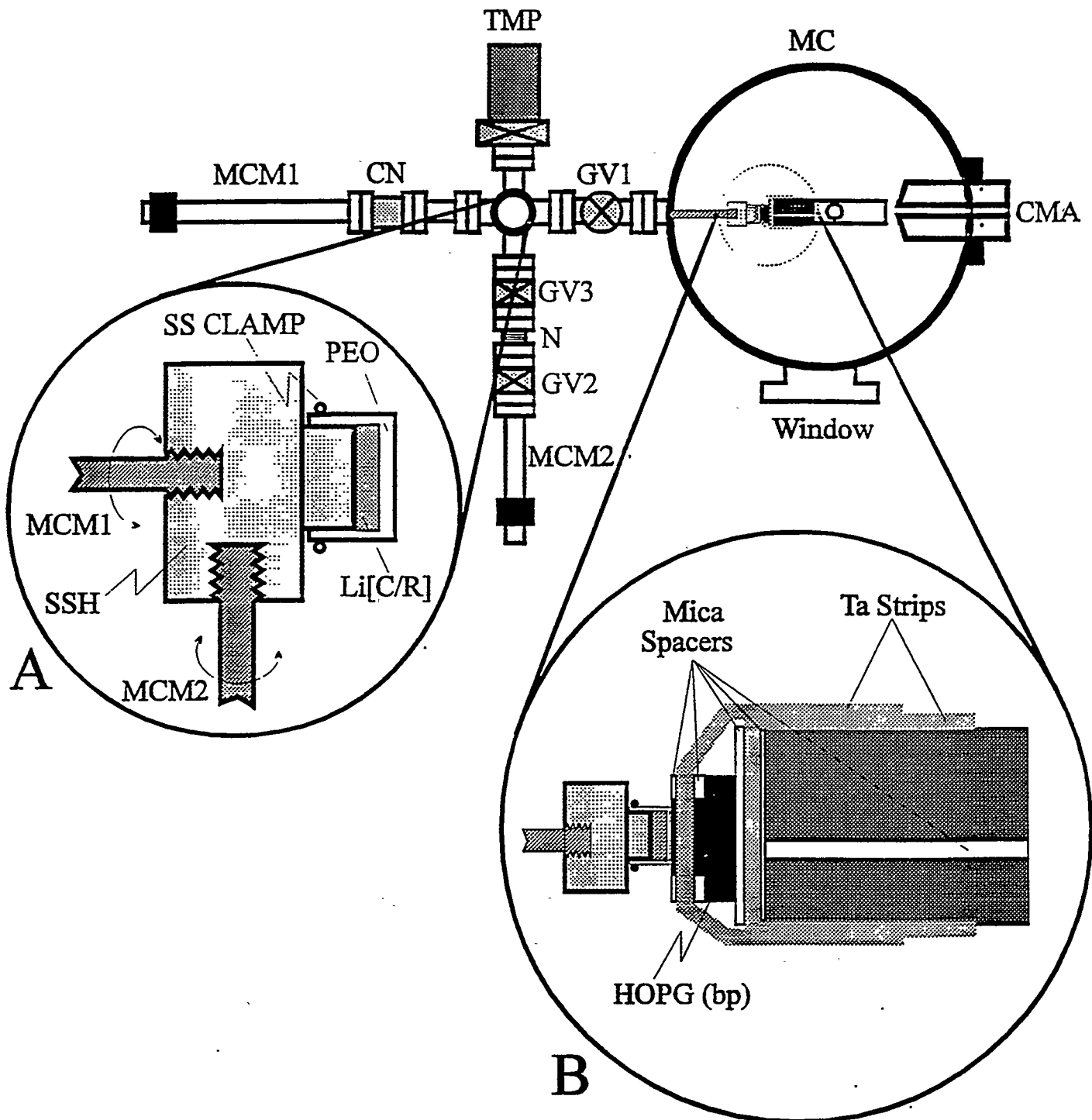


Figure 1

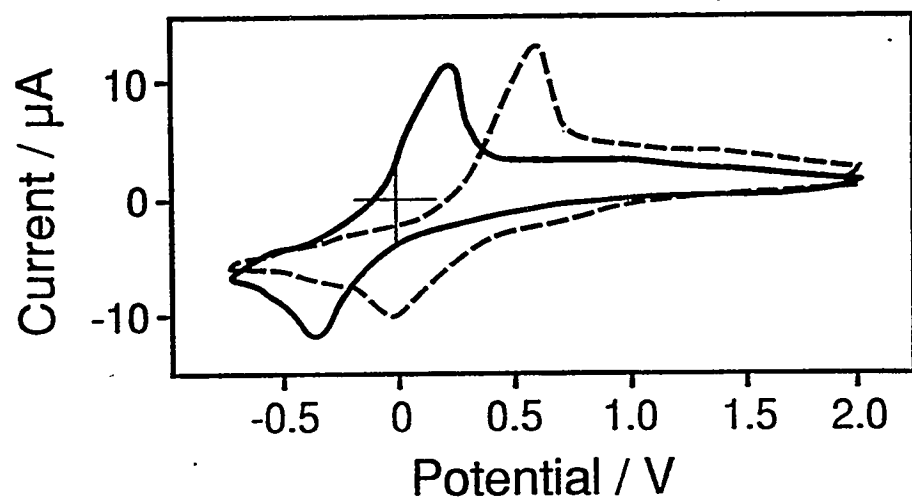


Figure 2

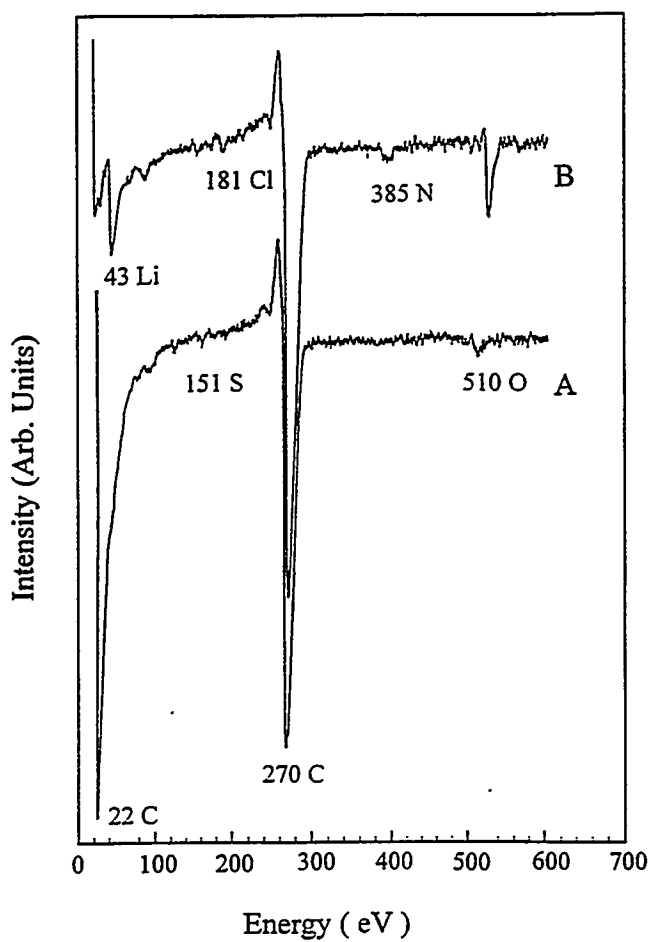


Figure 3

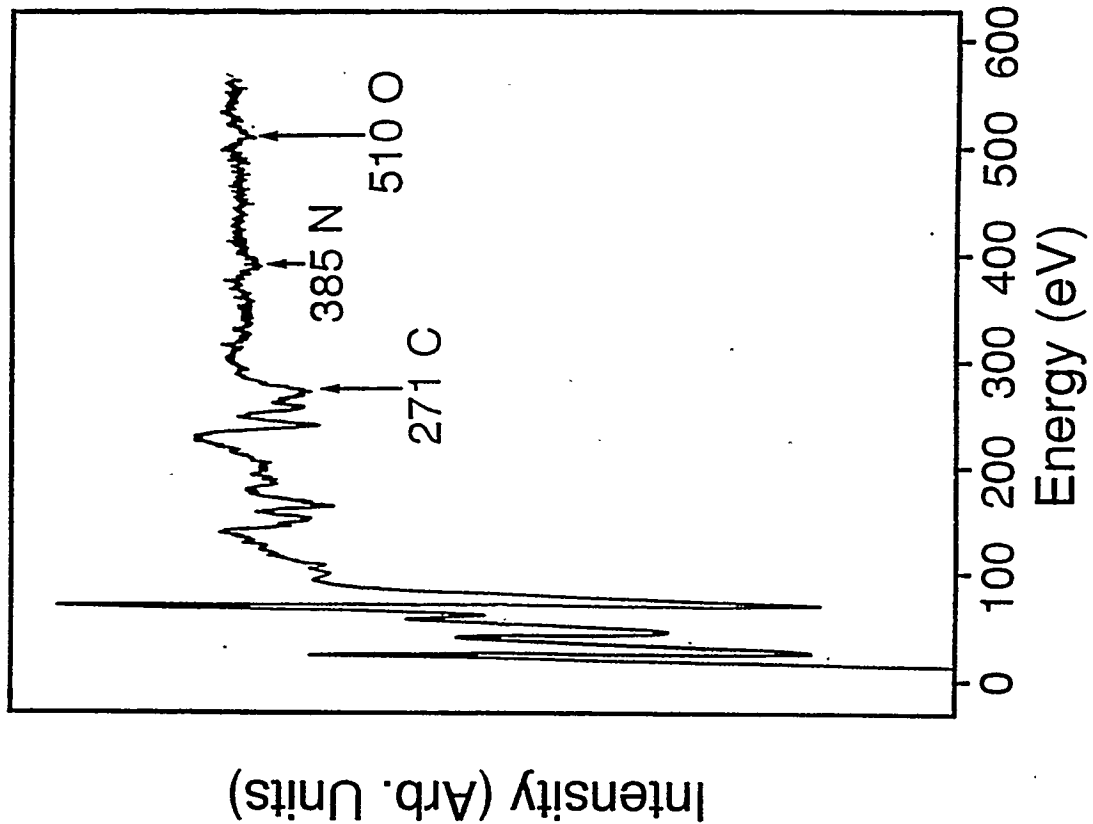


Figure 5

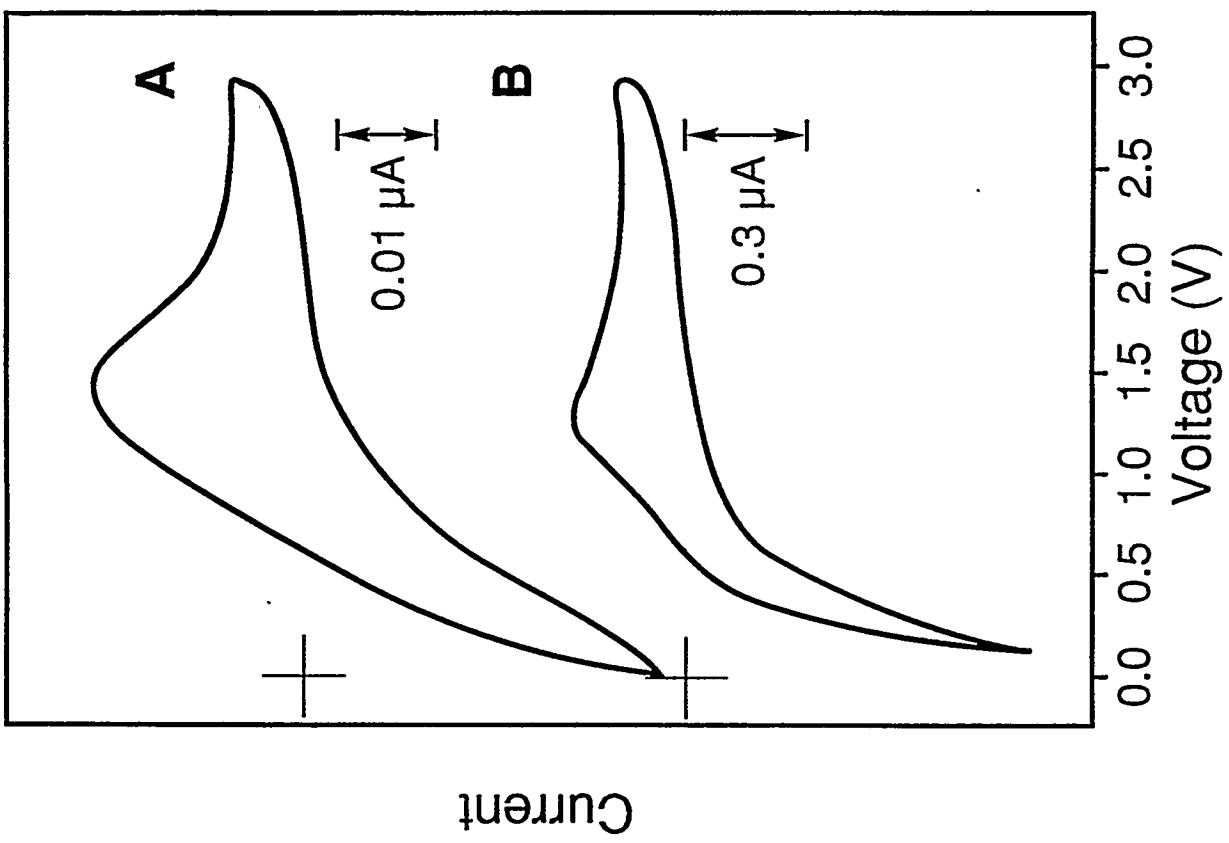


Figure 4

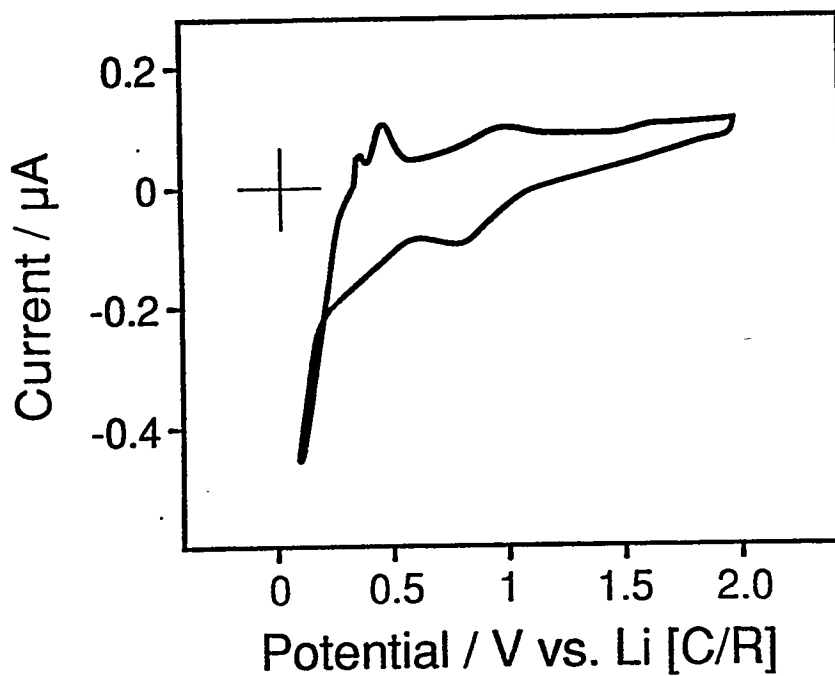


Figure 6

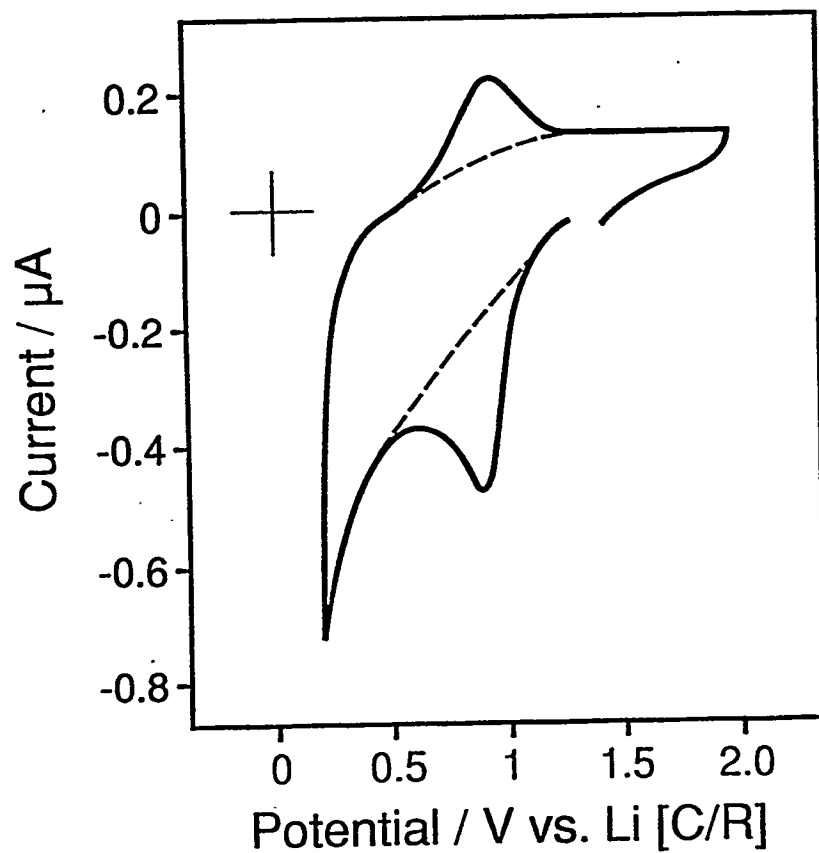


Figure 7

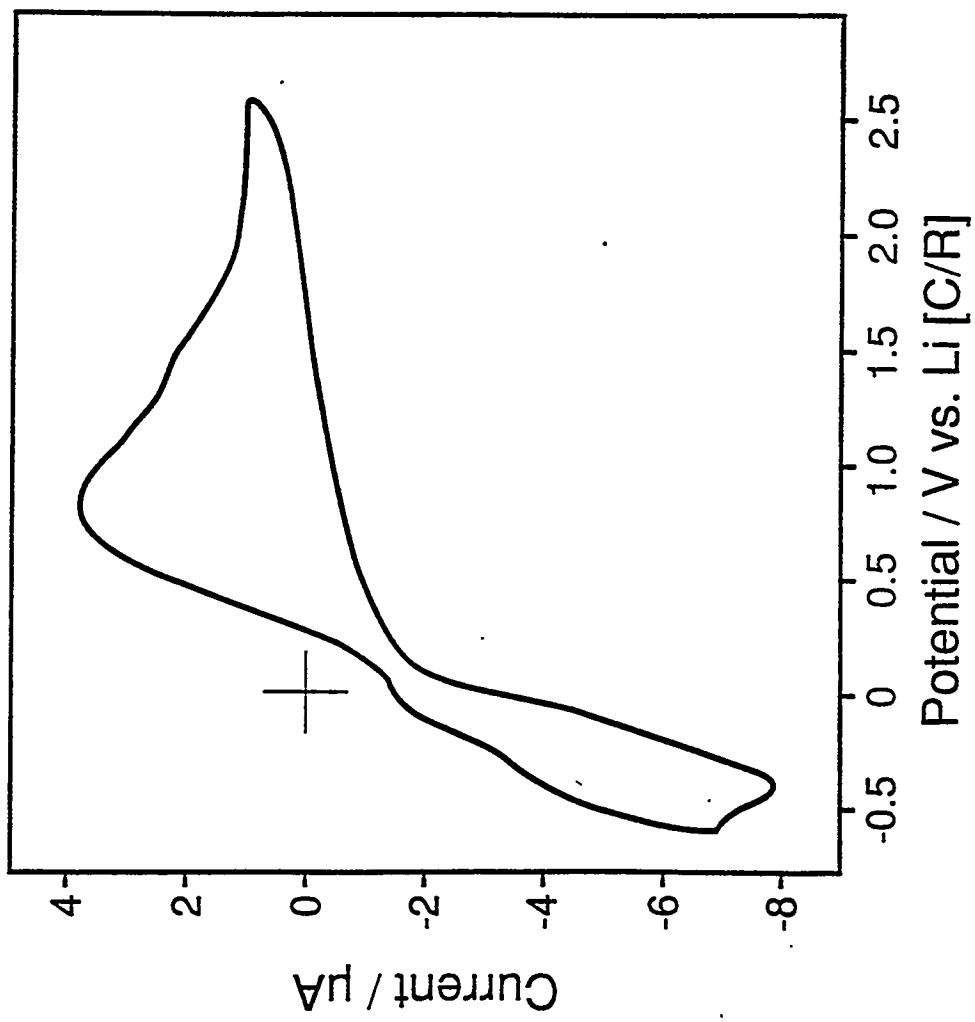


Figure 9

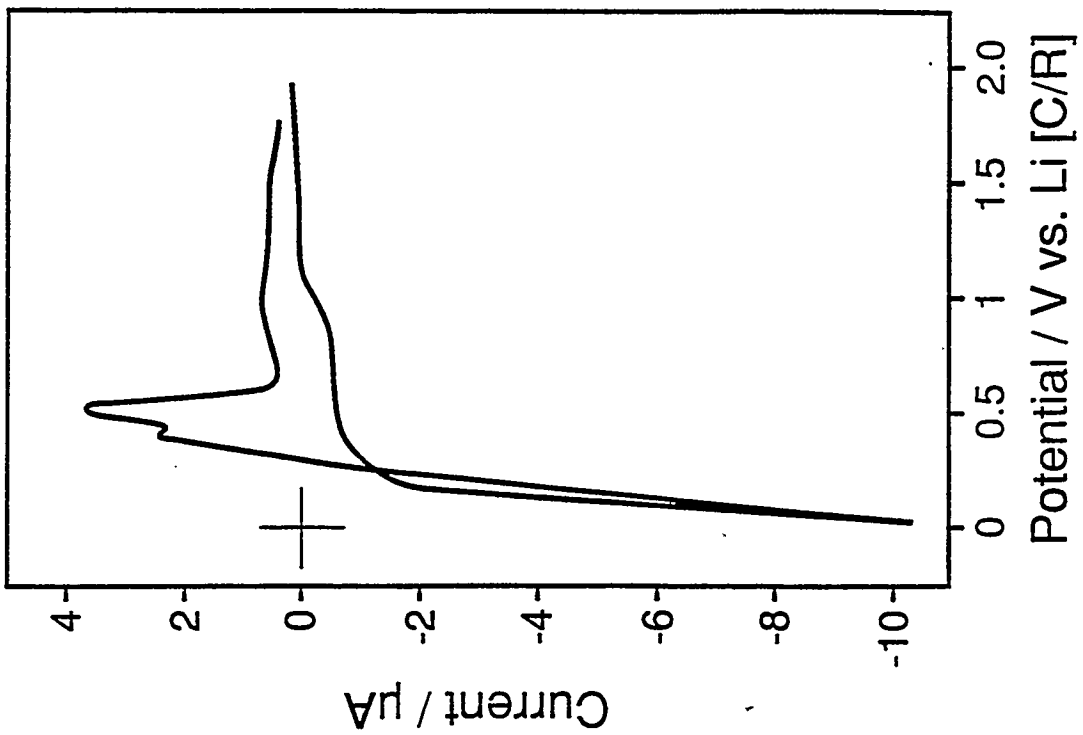


Figure 8